Chemically Induced Dynamic Electron Polarization Study on the Mechanism of Exchange Interaction in Radical Ion Pairs Generated by Photoinduced Electron Transfer Reactions

Yasuhiro Kobori,[†,‡] Shinji Sekiguchi,[†] Kimio Akiyama,[†] and Shozo Tero-Kubota*[,†]

Institute for Chemical Reaction Science, Tohoku University, Sendai, 980-8577, Japan, and PRESTO, Japan Science and Technology Corporation (JST), Kawaguchi, Japan

Received: February 1, 1999; In Final Form: April 29, 1999

Photoinduced electron transfer reactions were studied by using the continuous wave time-resolved electron paramagnetic resonance and Fourier-transformed electron paramagnetic resonance spectroscopy in polar solvents. The chemically induced dynamic electron polarization was investigated in both singlet and triplet precursor intermolecular electron transfer systems. The signs of the exchange interaction, which are defined by the energy differences between the singlet and triplet radical ion pairs, depended on the free energy changes for the charge recombination processes. The results are interpreted in terms of the mechanism that the spin selective stabilization and destabilization are caused by the perturbation through the electronic coupling from the ground state and the locally excited triplet state of the donor−acceptor pair at the equilibrium nuclear coordinate. In the singlet precursor electron transfer systems, the positive exchange interaction resulted from the selective triplet stabilization in the radical ion pair, when the ion pair state crossed with the locally excited triplet state at the normal region. In the triplet precursor electron transfer systems, the negative exchange interaction resulted from the selective singlet stabilization when the ion pair state crossed with the singlet ground state at the normal region. When the free energy change is larger than about 1.8 eV, the positive exchange interaction resulted from the spin-selective destabilization in the singlet ion pair, since the level crossing occurs at the inverted region.

Introduction

Exchange interaction (J) between two paramagnetic molecules is quite important to clarify the nature of the intermediates and mechanistic details of the reactions. The J is defined as the energy splitting between the singlet and triplet radical pairs (RPs) and has been considered to be due to the effect of the valence bonding interaction within the intermediate RPs,[1]

$$2J = E_S(\mathrm{RP}) - E_T(\mathrm{RP}) \quad (1)$$

where E_S(RP) and E_T(RP) represent the energies of the singlet and triplet RPs, respectively. According to the Heitler−London model, the singlet RP is stabilized and the triplet RP is destabilized since the exchange integral is negative with an overlap of the unpaired electron orbital in the randomly oriented two molecules, $J < 0$ in eq 1.[2]

Observations of the chemically induced dynamic nuclear polarization (CIDNP) and chemically induced dynamic electron polarization (CIDEP) enable us to investigate details of the photochemical reaction dynamics.[1,3] According to the radical pair mechanism (RPM),[1,3] when the g value difference between the two radicals is quite small, the singlet−triplet mixing (S−T_0 mixing) is induced through the hyperfine interaction (HFI). The nuclear and electron spin polarization is generated by the S−T_0 mixing during the diffusive separation and the possible subsequent reencounter of the two radicals, where the magnitude of the J is comparable to the magnitude of the HFI.[1,3] The CIDEP spectra due to the RPM are dependent on the spin multiplicity of the reaction precursor states (singlet or triplet) and the signs of the exchange interaction. For example, in the case of the triplet precursor, the CIDEP spectrum of a radical shows the microwave emission (E) in the lower magnetic field, and the absorption (A) in the higher field (E/A pattern), when the J is negative. If the J is positive with the triplet precursor, the phase of the RPM spectrum is inverted and the A/E pattern is obtained. The signs of the J in RPs are determined from the phases of the mutiplet (E/A or A/E) effects of the RPM polarization if the reaction precursor states are known.

In the liquid phase intermolecular systems of the neutral radical pairs and radical−triplet pairs,[4,5] almost all of the experimental results showed the negative exchange interactions and have been consistent with the Heitler−London model. On the contrary, in the photoinduced electron transfer reaction systems, there have been several reports that the sign of the J shows positive ($J > 0$) in some radical ion pairs; that is, the singlet ion pairs have the higher energies than the triplet ones.[6−10] One of the most puzzling subjects has been that the signs of the J vary with the species in the donor−acceptor systems in the triplet precursor reaction systems.[9,11] The positive exchange interactions were also obtained in the radical ion pairs generated via the singlet exciplexes.[6] Batchelor et al.[6] observed the CIDEP spectra in the system of the photoinduced electron transfer reactions of aromatic hydrocarbons. The CIDEP spectra were the E/A patterns with the excited singlet quenching, and the positive Js were concluded in the radical ion pairs. However, a careful analysis is needed for the determination of the precursor spin multiplicity. There is a possibility that the precursor of the multiplet polarization might be due to the minor triplet route with $J < 0$, as suggested in the recent studies.[12]

There are some mechanisms proposed about the signs of the exchange interaction in the radical ion pairs. According to the

[†] Tohoku University.
[‡] Japan Science and Technology Corp.

10.1021/jp990359d CCC: $18.00
Published on Web 06/24/1999

SCHEME 1

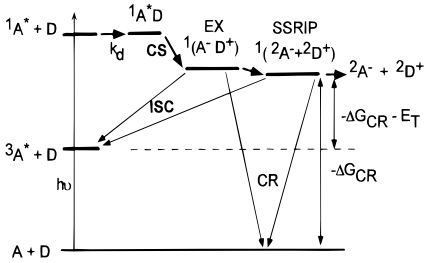

McConnell mechanism,[13] the positive exchange interaction is obtained by the perturbation from the triplet state of the pair of the doubly-charged donor and acceptor. Adrian[1] proposed that the energy shift of the singlet or triplet radical ion pair may occur by the mechanism that the ion pair wave functions acquire a small component of the locally excited states of the donor−acceptor complex with the electronic interaction. Volk et al. suggested, in the photosynthetic reaction centers, that the energy difference between the singlet and triplet primary radical ion pairs (P^+H^-) is determined by the electronic interaction from the singlet and triplet states $^1P^*$ and $^3P^*$ at the equilibrium nuclear configuration of the P^+H^-.[14] In our previous study, we briefly reported that the sign of the J is dependent on the charge recombination free energy in polar solvents.[10a,b] Experimental results indicated that the singlet radical ion pair energy is selectively shifted by the perturbation from the ground state encounter complex through the charge transfer (CT) interaction at the equilibrium solvent coordinate.

Thus far, some mechanisms[6,8,10,17,18] have been proposed to explain the opposite phases of the RPM CIDEP spectra to the phases obtained in the case of $J < 0$. However, a general mechanism of the exchange interaction has not been established in the radical ion pair of the liquid phase intermolecular system. In this paper, CIDEP spectra of ion radicals were observed in the several bimolecular photoinduced electron transfer reaction systems by using the continuous wave time-resolved electron paramagnetic resonance (CW-TREPR) and the Fourier-transformed electron paramagnetic resonance (FT-EPR) spectroscopy at room temperature. To determine the signs of the J, we analyzed the origin of the CIDEP mechanisms and the precursor spin multiplicities of the geminate radical ion pairs for the observed multiplet CIDEP signals. The determined signs of the J are shown to be strongly dependent on the energy gaps ($-\Delta G_{CR}$, the free energy changes for the charge recombination processes) expressed in polar solvents, as follows

$$-\Delta G_{CR} = E_{1/2}{}^{ox} - E_{1/2}{}^{red} - C \qquad (2)$$

where $E_{1/2}{}^{ox}$ and $E_{1/2}{}^{red}$ represent the oxidation and reduction potentials of the donor and the acceptor in polar solvents, respectively. C denotes Coulomb attraction energy within the ion pair.

First, the RPM CIDEP with the singlet precursor electron transfer reactions in the systems of aromatic hydrocarbons is discussed. In these systems, the energies of the $-\Delta G_{CR}$ are larger than the energies (E_T) of excited triplet states of aromatic hydrocarbons as shown in the energy diagram in Scheme 1. After the charge separation (CS) reactions occur from the encounter complexes of the fluorescent singlet molecules and electron donors, the singlet exciplexes (EX) are formed.[19] The ion radicals are separated to form the solvent-separated radical ion pairs (SSRIP) via the singlet exciplexes. After the intersystem crossing (ISC) of the exciplexes, the charge recombination process yields excited triplet states of the acceptor or donor.[20] The transient ion radicals are terminated by the charge recombination (CR) process. The CIDEP is observed on the free ion radicals which escape from the SSRIPs.

SCHEME 2

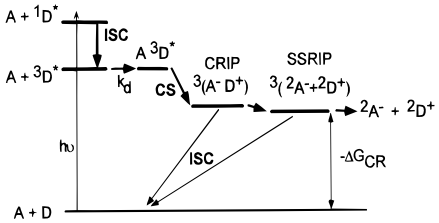

Second, the RPM CIDEP generated by the triplet quenching electron transfer reactions is discussed. TREPR spectra observed in the systems of *N*-methylphenothiazine as an electron donor and several electron acceptors were investigated. In these systems, ISC of the first excited singlet state is so fast that the S_1 molecules cannot encounter the quencher molecules by the diffusion motion. The $-\Delta G_{CR}$ energy is smaller than the E_T energy, and thus the charge separation occurs from the excited triplet state as shown in Scheme 2. The SSRIP is formed via the contact radical ion pair (CRIP). The charge recombination yields the ground state molecules after the ISC from the radical ion pairs. We propose a general mechanism called charge-transfer type exchange interaction, which explains almost all of the experimental results.

Experimental Section

The FT-EPR measurements were carried out using an X-band pulsed EPR spectrometer (Brucker ESP 380E) equipped with the dielectric resonator with a low Q factor of about 100. The microwave was amplified by a 1 kW TWT amplifier and the sequence was triggered by the synchronous output of a Nd:YAG laser (Quanta-Ray GCR-150, 30Hz, ~6 ns duration). To prevent the dead time problem in the detection of the free-induction decay, we employed a two-pulse ($\pi/2-\tau-\pi$) echo sequence with a CYCLOPS phase cycling routine and obtained the FT-EPR spectra.[21] The echo signals were accumulated by the digital storage oscilloscope (LeCroy Model 9450A) synchronized with the microwave pulse programmer. Time resolution of our FT-EPR measurements was determined by the width of the $\pi/2$ pulse, and was 16 ns in the present experiments. The steady-state CW-EPR spectra were measured with the 100 kHz field modulation.

The CW-TREPR measurements were performed with a Varian E-109E X-band EPR spectrometer without field modulation. Transient EPR signals generated by the pulsed laser irradiation were detected by the diode of the EPR spectrometer and transferred to a boxcar integrator (NF Model BX-531) for the time-resolved EPR spectra. A wide band amplifier was inserted between the detection system and the signal analyzer. The frequency of microwave and the strength of magnetic field were measured by a microwave counter (Echo Electronics EMC-14) and an NMR field meter (Echo Electronics EFM-2000AX), respectively. The third harmonics (355 nm) of the Nd:YAG laser was used for the excitation light source in both the FT and CW-EPR measurements. All solutions were deoxygenated by passage of Ar gas for 30 min and flowed into a quartz tube (4 mm od) for the FT-EPR measurements and a quartz flat cell (0.5 mm interior space) for the CW-TREPR measurements. All spectra were measured at room temperature.

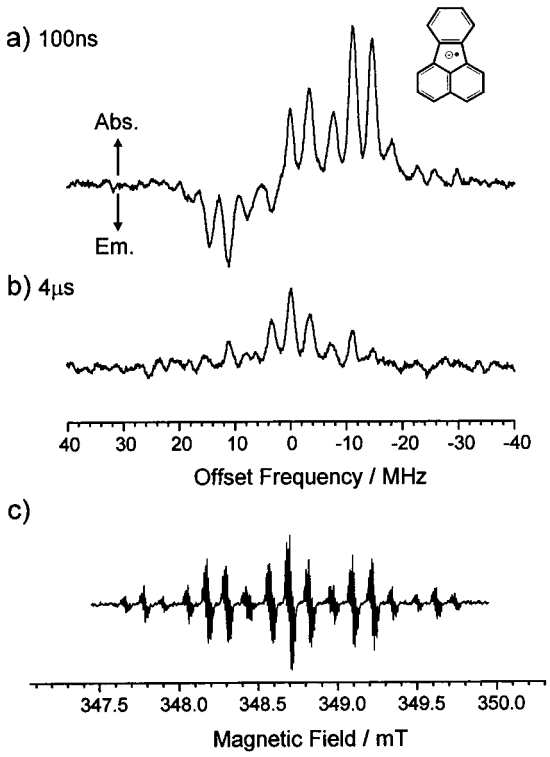

Figure 1. Echo-detected FT-EPR spectra of fluoranthene anion radical obtained at (a) 100 ns and (b) 4 μs after the 355 nm laser excitation in the fluoranthene (0.6 mM)−DMA (15 mM) system in 3:1 v/v mixture of cyclohexanol and acetonitrile. (c) Steady state CW-EPR spectrum of fluoranthene anion radical.

Results

RPM CIDEP Generated by Singlet Quenching Electron Transfer of Aromatic Hydrocarbons. In Figure 1, echo detected FT-EPR spectra observed at (a) 100 ns and (b) 4 μs after the 355 nm laser excitation are shown in the system of fluoranthene-*N*,*N*-dimethylaniline (DMA) in the 3:1 v/v mixture of cyclohexanol and acetonitrile. These spectra were assigned to fluoranthene anion radical by the g value (g=2.0026) and the hyperfine structure of the radical obtained by the steady state CW-EPR measurement of fluoranthene anion radical produced by the reduction of fluoranthene with potassium as shown in Figure 1c. Absence of the signal of the counter cation radical may be due to the fast spin-spin relaxation of $DMA^{+\bullet}$, or the broadening by the degenerate electron transfer between $DMA^{+\bullet}$ and DMA added with high concentration. The phase of the RPM CIDEP contribution in Figure 1a was determined to be the E/A type on the basis of the absorptive thermal equilibrium signal observed at 4 μs in Figure 1b. In Figure 1a, the additional absorptive polarization to the E/A one is caused by the effect of the g value difference (Δg mechanism)[1] in the RPM, since the g value of $DMA^{+\bullet}$ is reported to be 2.0033[6] which is larger than that of the anion radical. The CIDEP from the triplet mechanism (TM)[3b] is not involved in the observed signal, suggesting no contribution from the triplet reaction channel on the CIDEP generation.

To determine the precursor spin state for the generation of the E/A type polarization, dependence of the FT-EPR spectra on the delay time (τ_d) between the laser pulse and $\pi/2$ pulse was measured under the conditions of 5 mM < [DMA] < 25 mM (Figure 2a). The contribution of the multiplet E/A effect was obtained from intensity difference between the signals at ±14.6 MHz in Figure 1a. In Figure 2a, the time profiles of the RPM contribution were fitted with the simulated time dependence of the RPM contribution. The time development of the RPM signal is represented as follows[21b]

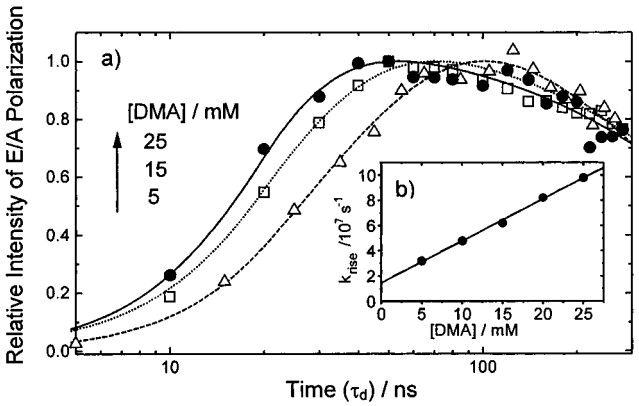

Figure 2. (a) DMA concentration effect on the time profiles of the E/A type multiplet contribution observed on fluoranthene anion radical. (b) Stern−Volmer plot of the signal rise of the multiplet contribution against [DMA].

$$F(\tau_d) = \exp(k_{rise}\,\tau_d) - \exp(\tau_d/T_1) \quad (3)$$

where

$$k_{rise} = 1/\tau_0 + k_{ET}[\mathrm{DMA}] \quad (4)$$

In eq 3, k_{rise} and T_1 represent the buildup rate of the RPM signals due to the charge separation reaction and the spin−lattice relaxation time of the radical, respectively. τ_0 denotes the lifetime of the excited state and k_{ET} the rate constant of the charge separation reaction from DMA to the excited state. The function $F(\tau_d)$ was convoluted with the response function determined by the width of the $\pi/2$ pulse (τ_R = 16 ns in the present experiment) to obtain the simulated time profiles $S(\tau_d)$ in Figure 2a, assuming the response function to be exponential

$$S(\tau_d) = \int_0^\infty \exp(-t/\tau_R) F(\tau_d - t)\,\mathrm{d}t \quad (5)$$

From the least-squares fits by eqs 3 and 5, the T_1 value was obtained to be 0.7 μs and was not influenced by the DMA concentration. In Figure 2b, Stern−Volmer plot of k_{rise} versus DMA concentration is shown. From eq 4, $k_{ET} = 3.3(\pm 0.1) \times 10^9$ M^{-1} s^{-1} and $1/\tau_0 = 1.5(\pm 0.2) \times 10^7$ s^{-1} were obtained. The deactivation rate of the S_1 state fluoranthene was determined by the time-resolved emission spectroscopy in the same solvent to be 1.8×10^7 s^{-1} which is consistent with the reported value.[22] The $1/\tau_0$ value obtained above agrees well with the fluorescence deactivation rate of the S_1 state, and therefore, the precursor of the E/A polarization is the first excited singlet state. This result is well consistent with the Rehm−Weller relation.[23] The rate constant of the charge separation reaction is dependent on the free energy change (ΔG_{CS}) to form a pair of separated ions ($A^- + D^+$) from a pair of excited neutral donor−acceptor ($A^* + D$) as

$$\Delta G_{CS} = E_{1/2}{}^{ox} - E_{1/2}{}^{red} - E_A{}^* - C \quad (6)$$

where $E_A{}^*$ is the excited state energy. Ignoring the Coulomb term in eq 6 as a small contribution, ΔG_{CS} is calculated to be positive ($\Delta G_{CS} = +0.20$ eV) in the case of the T_1 quenching, while $\Delta G_{CS} < 0$ ($\Delta G_{CS} = -0.57$ eV) in the case of the S_1 quenching (see Supporting Information). These results show that the reaction predominantly occurs from the S_1 state. The viscosity of the 3:1 v/v mixture of cyclohexanol and acetonitrile

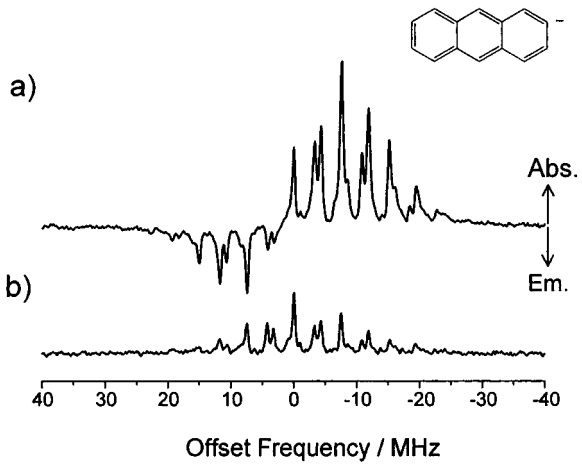

Figure 3. Echo-detected FT-EPR spectra of the center part of anthracene anion radical obtained at (a) 100 ns and (b) 4 μs in the anthracene (0.45 mM)−DMA (100 mM) system in 3:1 v/v mixture of cyclohexanol and acetonitrile.

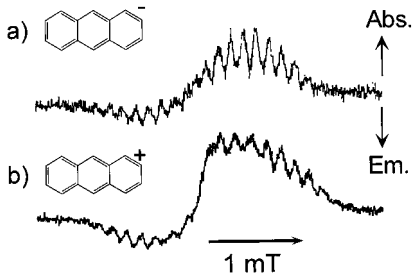

Figure 4. CW-TREPR spectra of (a) anthracene anion radical obtained in the anthracene (2 mM)−DMA (100 mM) system in the 3:1 v/v mixture of cyclohexanol and acetonitrile and (b) anthracene cation radical in the anthracene (2 mM)−1,4-DCNB (100 mM) system in dimethyl sulfoxide obtained at 0.5 μs after the 355 nm laser excitation.

is reported to be 3 cP at room temperature.[19] The k_{ET} (=3.3 × 10^9 M^{-1} s^{-1}) obtained is well comparable to the diffusion-controlled rate constant[22] under the 3 cP viscosity of the solvent. This result strongly supports that the E/A type polarization is generated by the singlet quenching reaction originated from the geminate radical ion pair. From the above experimental results, CIDEP spectra generated by the singlet precursor reactions can selectively be observed when the triplet state energies are smaller than the energies of the ion pair states, i.e., $E_T < -\Delta G_{CR}$ (see Scheme 1).

We observed the CIDEP spectra in the other donor−acceptor systems of the singlet precursor reaction systems. Figure 3 shows the FT-EPR spectra of the center part of the anthracene anion radical observed with the quenching of excited anthracene by the electron donor DMA. Hyperfine structure was well reproduced with the reported hyperfine coupling constants of 0.5337 (2H), 0.2740 (2H), and 0.1509 (2H) mT.[25] Also, the charge separation hardly occurs from the anthracene T_1 state since the ΔG_{CS} (=+0.81 eV) is quite larger than the ΔG_{CS} = +0.20 eV in the fluoranthene−DMA system in the case of the T_1 quenching.[22,24] As was seen in the fluoranthene−DMA system, the E/A type RPM CIDEP was also observed on anthracene anion radical with the singlet quenching reaction as shown in Figure 3a. With the CW-TREPR measurement, the same CIDEP pattern as obtained by the FT-EPR measurement was observed in the anthracene−DMA system (Figure 4a). The E/A pattern was also observed with the oxidation of anthracene by electron acceptors. Figure 4b shows a CW-TREPR spectrum of anthracene cation radical obtained with the quenching of the excited anthracene by 1,4-dicyanobenzene (1,4-DCNB). The hyperfine structure was well reproduced with the reported hyperfine coupling constants of 0.6533 (2H), 0.3061 (2H), and 0.1379 (2H) mT.[25] The oxidation potential of anthracene, the reduction potential of 1,4-DCNB, and the triplet state energy of anthracene yield the positive ΔG_{CS} (=+0.92 eV) in the case of T_1 quenching. Therefore, the E/A pattern is also originated from the excited singlet state.

We also observed the FT-EPR spectra in the systems of fluoranthene-4-bromo-*N*,*N*-dimethylaniline (4BrDMA), fluoranthene-1,2,4,5-tetracyanobenzene (1,2,4,5-TCNB), fluoranthene-1,2,4-trimethoxybenzene (1,2,4-TMB), coronene−DMA, anthracene-1,2-DCNB, and dibenz[*a*,*h*]anthracene-DMA in the 3:1 v/v mixture of cyclohexanol/acetonitrile. In these systems, the excited triplet energies are also smaller than the $-\Delta G_{CR}$ ones. Table 1 summarizes the results of the RPM phases on the ion radicals obtained in the singlet precursor reaction systems together with the reported ones.[6] The E/A type RPM polarization was observed on the ion radicals that can energetically be generated only from the S_1 states. Since the E/A type geminate pair RPM polarization is generated with the S_1 precursor, the signs of the exchange interaction seem not to be negative but positive ($J > 0$) in the radical ion pairs. Details about the determination of the signs of the J are discussed later.

RPM CIDEP Generated by Triplet Quenching Electron Transfer. Figure 5 shows the CW-TREPR spectra obtained by the 355 nm laser excitation of *N*-methylphenothiazine in the presence of electron acceptors of (a) 1,2,4,5-TCNB in the 4:1 (v/v) mixture of dimethyl sulfoxide (DMSO)−glycerol and (b) 1,4-DCNB in DMSO, respectively. The CIDEP spectrum in the *N*-methylphenothiazine−1,4-DCNB system (Figure 5b) agrees with that reported by Sakaguchi et al.[26] The broad peaks were assigned to *N*-methylphenothiazine cation radical and the sharp ones to 1,4-DCNB anion radical ($DCNB^{\bullet-}$). In the CIDEP spectrum of Figure 5a, the cation radical is also observed and sharp peaks are assigned to the anion radical of $TCNB^{\bullet-}$ which was reproduced with the reported hyperfine coupling constants ($a^H = 0.111$ mT (2H) and $a^N = 0.115$ mT (4N)).[27] Investigation of a transient absorption measurement clearly showed the electron-transfer reactions are originated from the excited triplet *N*-methylphenothiazine.[26] It is obvious that the CIDEP spectra are different from each other in the phase; the RPM polarization shows the E/A type in Figure 5a, while it shows A/E in Figure 5b. The CIDEP spectra of both cation and anion radicals were simulated with the square root dependence of the RPM CIDEP on the difference (Q_{ab}) between the resonance Larmor frequencies of the two radicals based on the conventional RPM theory.[1] Simulations of the CIDEP spectra are shown under the observed ones. In both spectra, the effect of the net emissive polarization due to the TM is added. Experimental results were well reproduced with $J < 0$ (E/A type polarization) in Figure 5a, while with $J > 0$ (A/E type polarization) in Figure 5b. The same RPM phases as in Figure 5, a and b, were respectively observed when phenothiazine was used as the donor. Experiments were also performed with the other electron acceptors of 1,2-DCNB, quinoxaline, 1,3-DCNB, 1,4-DCNB, phenazine, nitrobenzene, CCl_4, 1,2-dibromomethylbenzene (1,2-DBMB), and CBr_4. Results of the RPM phases and the signs of the J are listed in Table 2 together with the $-\Delta G_{CR}$ values calculated by the *N*-methylphenothiazine and phenothiazine oxidation potentials and the reduction potentials of the electron acceptors.[24] It is evident that the sign of the J depends on the $-\Delta G_{CR}$ value; the J is negative when $-\Delta G_{CR} < \sim 1.8$ eV, and is positive when $-\Delta G_{CR} > \sim 1.8$ eV. For example, the J is negative when

TABLE 1: Thermodynamic Parameters, Observed Phases of the Multiplet RPM Polarization, and the Signs of the Exchange Interaction in Radical Ion Pairs Generated by Singlet Quenching Electron Transfer Reactions of Excited Aromatic Hydrocarbons in Polar Solvents

fluorescer				quencher						
	$E_{1/2}^{red}$/V[a]	$E_{1/2}^{ox}$/V[a]	E_T/eV[b]		$E_{1/2}^{red}$/V[a]	$E_{1/2}^{ox}$/V[a]	$-\Delta G_{CR} - E_T$/eV[c]	RPM phase	sign of J	ref
fluoranthene	−1.78		2.29	DMA		0.71	+0.20	E/A	positive	this work
				4-BrDMA		0.86	+0.35	E/A	positive	this work
coronene	−2.07		2.37	DMA		0.71	+0.41	E/A[d]	positive	this work
anthracene	−1.95		1.85	DMA		0.71	+0.81	E/A	positive	this work
		1.09		1,4-DCNB	−1.68		+0.92	E/A	positive	this work
dibenz[*a*,*h*]anthracene	−2.04		2.26	DMA		0.71	+0.49	E/A	positive	this work
pyrene		1.16	2.10	1,3-DCNB	−1.88		+0.94	E/A	positive	6
		1.16		1,4-DCNB	−1.68		+0.74	E/A	positive	6
	−2.09			DMA		0.71	+0.70	E/A	positive	6

[a] Reference 24. [b] Reference 22. [c] Calculated from $-\Delta G_{CR} = E_{1/2}^{ox} - E_{1/2}^{red}$. [d] Obtained in DMSO.

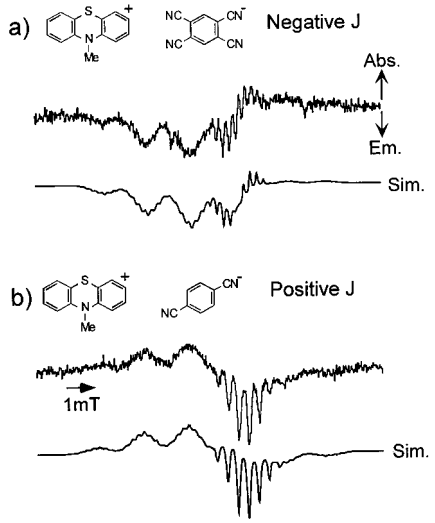

Figure 5. CW-TREPR spectra observed at 0.5 μs after the laser excitation of the systems of (a) *N*-methylphenothiazine (3 mM)−1,2,4,5-TCNB (5 mM) in 4:1 v/v mixture of DMSO and glycerol and (b) *N*-methylphenothiazine (3 mM)−1.4-DCNB (5 mM) in DMSO. Simulated CIDEP spectra are shown under the observed spectra.

$-\Delta G_{CR} = 1.37$ eV in the *N*-methylphenothiazine−1,2,4,5-TCNB system, while the J is positive when $-\Delta G_{CR} = 2.32$ eV in the *N*-methylphenothiazine−1,4-DCNB system in Figure 5. As far as we investigated, there were no exception results of the $-\Delta G_{CR}$ dependence of the J in the bimolecular electron transfer systems. There are many other CIDEP studies reported about the signs of the exchange interaction generated by the triplet precursor electron transfer reactions in the polar solvents as listed in Table 3.[9,11,28−31] Similar dependence of the signs of the exchange interaction on the $-\Delta G_{CR}$ is also seen in the previously reported systems.

Discussion

Assignment of the Multiplet RPM CIDEP: Contributions of the Exchange and Dipole−Dipole Interactions. Recently, a novel mechanism has been proposed for the generation of the multiplet CIDEP originated from the radical ion pair. Shushin[17] theoretically demonstrated an electron dipole−dipole interaction (DDI) also induces the multiplet polarization in the liquid phase. A long-range $S-T_0$ mixing induces the DDI polarization where the magnitude of the J is quite smaller than that of the HFI. The RPM phase due to the DDI mechanism is the same as the conventional RPM phase with $J > 0$. At first, before we determine the signs of the J, we must determine the origin of the multiplet CIDEP mechanism for the observed CIDEP spectra. The contribution of the DDI mechanism was estimated to be much smaller than that from the RPM induced by the exchange interaction J.[18] Shkrob[18] demonstrated that the DDI mechanism cannot be applied in the systems of radical ion pairs generated via the exciplex or the contact radical ion pair. In the systems in Table 1, the long-range charge separation reactions hardly occur, since, as studied by Kikuchi et al., the energy gaps (ΔG_{CS}) are smaller than 1 eV for the charge separation reactions from the S_1 states.[33] The short-range spin exchange will dominantly occur in the singlet geminate radical pairs. This is confirmed from the results that the obtained rate constant k_{ET} of the charge separation reaction is diffusion limited in the fluoranthene−DMA system, and, as in Scheme 3, the charge recombination rate (k_S) of the singlet geminate radical ion pair is smaller than that (k_T) of the triplet pairs (see Supporting Information).

The DDI contribution is also eliminated in the triplet precursor reaction systems in Figure 5. Shkrob[18] calculated the Q_{ab} dependence of the DDI-induced multiplet polarization P_{DDI}, and obtained that the P_{DDI} is not proportional to square root of Q_{ab}; instead, $P_{DDI} \propto Q_{ab}$ or $P_{DDI} \propto Q_{ab}^{-1}$ was obtained. The CIDEP spectra of both *N*-methylphenothiazine cation and cyanobenzene anion radicals were simulated by the conventional square root dependence[1] of the RPM polarization on the Q_{ab} values, as shown in Figure 5. The good agreement between the experimental results and the simulations demonstrates that the J-induced multiplet polarization dominates the observed CIDEP. The obtained phases of the multiplet RPM CIDEP are not governed by the DDI but the signs of the J in the radical ion pairs. Determined signs of the J are listed in Table 1−3. Details of the determination of the signs of the J are described in the Supporting Information.

Mechanism of Charge-Transfer Type Exchange Interaction in Radical Ion Pairs. In the ionic radical pair systems, the charge recombination reactions to the ground states and to the locally excited triplet states occur as in Scheme 1 and 2. According to the electron transfer reaction theory, the equilibrium nuclear configuration (nuclear coordinate) of the solvent and solute molecules is different between the neutral and charged donor−acceptor pairs in the polar solvents.[15,16] It is well-known that the effect of the solvent and solute reorganizations has an important role to determine the electron transfer reaction rate.[15,16] To completely explain the energy gap dependence of the signs of the J, we propose a mechanism of the charge-transfer type exchange interaction which is taken into account the equilibrium change of the solvent and solute nuclear coordinate.

Here, as in Figure 6, we propose a consecutive dependence of the signs of the J on the energy gaps of $-\Delta G_{CR}$ in the systems of the bimolecular electron transfer reactions. In the left side

TABLE 2: $-\Delta G_{CR}$ Dependence of the Signs of the Exchange Interaction in Radical Ion Pairs Determined from the Phases of the Multiplet RPM Polarization Generated by the Triplet Precursor Electron Transfer Reactions of Phenothiazine and *N*-Methylphenothiazine in DMSO

donor		acceptor				
	$E_{1/2}^{ox}$/V[24]		$E_{1/2}^{red}$/V[24]	$-\Delta G_{CR}$/eV[a]	RPM phase	sign of J
N-methylphenothiazine	0.64	1,3-DCNB	−1.88	2.52	A/E	positive
		1,2-DCNB	−1.83	2.47	A/E	positive
		quinoxaline	−1.70	2.34	A/E	positive
		1,4-DCNB	−1.68	2.32	A/E	positive
		phenazine	−1.23	1.87	A/E	positive
		nitrobenzene	−1.08	1.72	E/A	negative
		CCl_4	−0.78	1.42	E/A	negative
		1,2,4,5-TCNB	−0.73	1.37	E/A	negative
		1,2-DBMB	−0.61	1.25	E/A	negative
phenothiazine	0.56	1,3-DCNB	−1.88	2.44	A/E	positive
		1,2-DCNB	−1.83	2.39	A/E	positive
		1,4-DCNB	−1.68	2.24	A/E	positive
		1,2,4,5-TCNB	−0.73	1.29	E/A	negative
		1,2-DBMB	−0.73	1.17	E/A	negative
		CBr_4	−0.3	0.86	E/A	negative

[a] Calculated from $-\Delta G_{CR} = E_{1/2}^{ox} - E_{1/2}^{red}$.

TABLE 3: $-\Delta G_{CR}$ Dependence of the Signs of the Exchange Interaction Determined from the Phases of the Multiplet RPM Polarization with Triplet Precursor Reported in the Bimolecular Electron Transfer Reaction Systems in Polar Solvents

acceptor		donor					
	$E_{1/r}^{red}$/V[24]		$E_{1/r}^{red}$/V[24]	$-\Delta G_{CR}$/eV[a]	RPM phase	sign of J	ref
duroquinone	−0.73	ZnTPP	0.71	1.44	E/A	negative	11
		MgTPP	0.54	1.27	E/A	negative	28
		H_2TPP	0.95	1.68	E/A	negative	28
		Eosin Y	0.87	1.60	E/A	negative	29
		DMA	0.71	1.44	E/A	negative	30
		4-ClDMA	0.71	1.58	E/A	negative	30
		4-BrDMA	0.86	1.59	E/A	negative	30
		4-IDMA	0.86	1.56	E/A	negative	30
benzoquinone	−0.45	Eosin Y	0.87	1.32	E/A	negative	29
dichlorobenzoquinone	−0.18	Eosin Y	0.87	1.05	E/A	negative	29
benzophenone	−1.83	DABCO	0.68	2.51	A/E	positive	9
4-methoxybenzophenone	−1.74	DABCO	0.68	2.42	A/E	positive	9
4,4′-dimethoxybenzophenone	−2.02	DABCO	0.68	2.70	A/E	positive	9
maleic anhydride	−0.85	diphenylamine	0.83	1.68	E/A	negative	31
		triphenylamine	0.98	1.83	E/A	negative	31
		TMPD	0.32	1.17	E/A	negative	31
		9-methylcarbazole	1.16	2.01	A/E	positive	31
		9-ethylcarbazole	1.21	2.06	A/E	positive	31
		9-phenylcarbazole	1.12	1.97	A/E	positive	31

[a] Calculated from $-\Delta G_{CR} = E_{1/2}^{ox} - E_{1/2}^{red}$.

SCHEME 3

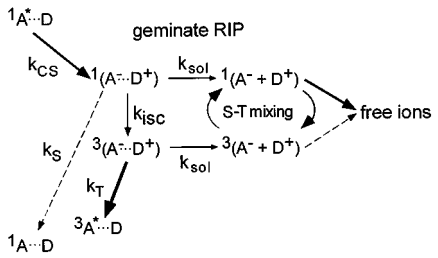

panels in (a−d) in Figure 6, parabola-shaped electronic potentials of the ground state donor−acceptor pair (^{1}A···D), radical ion pair ^{1,3}(A$^-$···D$^+$), locally excited triplet state (^{3}A*···D), and locally excited singlet state (^{1}A*···D) are plotted against the nuclear coordinate. In the right side panels that lie perpendicular to the left side panels, the potentials of the spin wave functions of the radical ion pairs are shown against the distance (r) between the ions. The solid and dotted lines show triplet and singlet spin multiplicity, respectively. The reorganization energy is represented as λ. It is noticeable that the equilibrium nuclear coordinate for ^{1,3}(A$^-$···D$^+$) is different from the coordinate for the neutral species and that the exchange interaction in the ^{1,3}(A$^-$···D$^+$) state is discussed at its equilibrium nuclear coordinate as indicated with energy axis on the left side panels in the figures. With a simple perturbation theory, the spin-selective energy shifts of the solvated ion pair states are caused by the perturbation from the ground state and the locally excited triplet state due to the electronic coupling at their equilibrium nuclear coordinates.

If values of the $-\Delta G_{CR}$, the reorganization energy (λ) and the triplet state energy (E_T) are known in the polar solvent, we are able to predict the sign of the J in a radical ion pair from Figure 6, and verify the experimental results.

(a) Singlet Precursor Reaction Systems. In the singlet precursor reaction systems in Table 1, the $-\Delta G_{CR}$ values are larger than the E_T ones and the energy differences between the ion pair states and the excited triplet states of the aromatic hydrocarbons are smaller than 1 eV; $-\Delta G_{CR} - E_T < 1$ eV. The reorganization energy λ is the energy required to reorganize the system to an optimum configuration for an electron transfer, and consists of a solvent component (outer-sphere reorganization energy, λ_S), and a component associated with the donor and

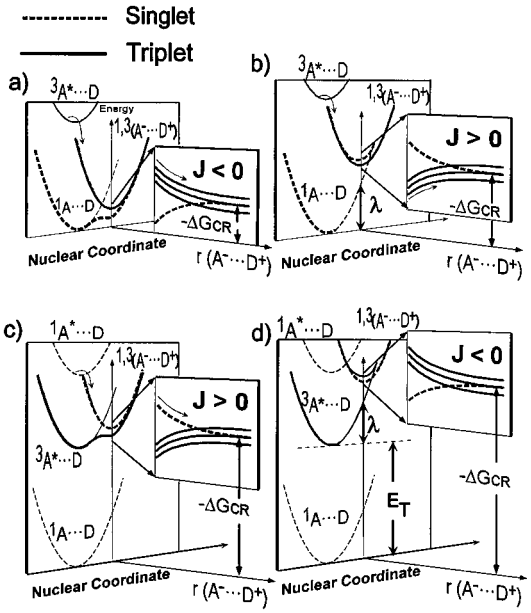

Figure 6. Schematic representation of the consecutive dependence of the singlet−triplet energy splitting in the solvated radical ion pairs, $^{1,3}(A^{-}\cdots D^{+})$, on the free energy change ($-\Delta G_{CR}$) for the charge recombination process. See text for discussion.

acceptor molecules (inner-sphere reorganization energy λ_V). The following Marcus relation represents the solvent reorganization energy λ_S in a polar solvent as[15]

$$\lambda_S = \frac{e^2}{2}\left(\frac{1}{r_A} + \frac{1}{r_D} - \frac{2}{r_{AD}}\right)\left(\frac{1}{n^2} - \frac{1}{\epsilon}\right) \qquad (7)$$

where r_D and r_A are radii of the reactants and r_{AD} is the distance between the donor and acceptor. n and ϵ represent refractive index and dielectric constant of solvents, respectively. Kikuchi et al.[33] estimated $\lambda_S \sim 1.6$ eV for the solvent-separated radical ion pairs. The λ_V energies were also estimated in these systems to be about 0.3 eV.[33] Thus, the total reorganization energy is estimated to be $\lambda = \lambda_S + \lambda_V \sim 1.9$ eV. Since the λ value is much larger than the $-\Delta G_{CR} - E_T$ values in the donor−acceptor systems in Table 1, the ion pair potentials cross with the locally excited triplet states at the normal region as shown in Figure 6c. The positive exchange interactions obtained in Table 1 are consistent with the model shown in Figure 6c. The singlet radical ion pairs selectively produced with the charge separation from the S_1 states are stabilized to the potential minimum of the ion pair state due to the reorganization in the solvent and solute molecules, as shown in the left side panel in Figure 6c. It is noted that the magnetic interaction operates at the nuclear coordinate of the potential minimum of $^{1,3}(A^{-}\cdots D^{+})$, because the reorganization occurs much faster than the time scale for the $S-T_0$ mixing in the radical ion pair. At the nuclear coordinate, triplet radical ion pair state $^3(A^{-}\cdots D^{+})$ is selectively stabilized by the perturbation from the locally excited triplet state $^3A^*\cdots D$ through the electronic coupling. The magnitude of the electronic coupling is governed by the orbital overlap in randomly oriented radical ion pair, and is dependent on the distance (r) between the radical ions. The singlet radical ion pair is not perturbed from the triplet locally excited state but from the ground state due to the spin selection rule for the charge recombination process. From Figure 6c, the triplet radical ion pair is more strongly perturbed from the locally excited triplet state than the singlet radical ion pair is perturbed from the ground state. This is consistent with the relation of $k_T > k_S$ in Scheme 3. As a result, potential energy surfaces of the radical ion pair are plotted against r as shown on the right side panel in Figure 6c, and thus, the positive exchange interaction results. All of the experimental results in Table 1 are consistent with the positive J in Figure 6c.

In the case of $-\Delta G_{CR} > E_T + \lambda$, the sign of the J is expected to be negative from Figure 6d. However, it is quite difficult to satisfy the energy relation in the bimolecular electron transfer reaction systems. To obtain the negative J with the singlet precursor, the energy difference between the S_1 and T_1 states of the aromatic hydrocarbon must be larger than the total reorganization energy λ. For example, S_1-T_1 energy difference of anthracene is only 0.95 eV, which is quite smaller than the energy of the λ (about 1.8 eV) in the polar solvents.

(b) Triplet Precursor Reaction Systems. In the triplet precursor reaction systems in Tables 2 and 3, because the $-\Delta G_{CR}$ values are smaller than the E_T ones, the energy relationships in Figure 6a,b are applicable. It is evident that the experimental results of the signs of the J are perfectly explained by the mechanism in the Figure 6a,b. The negative J is explained by Figure 6a. When the $-\Delta G_{CR}$ energy is smaller than the λ energy, the radical ion pair potential crosses with the ground state at the normal region. As described above, the singlet radical ion pair is selectively stabilized. The positive J is explained by Figure 6b; singlet radical ion pair is selectively destabilized, when the ion pair potential crosses with the ground state at the inverted region. The signs of the J were negative when $-\Delta G_{CR}$ values were smaller than about 1.8 eV, and were positive when $-\Delta G_{CR}$ values were larger than about 1.8 eV in Tables 2 and 3. It is noticeable that the boundary 1.8 eV is quite close to the total reorganization energy of λ roughly estimated above. There have been several optical studies that have estimated the reorganization energies in the donor−acceptor systems by the plots of the charge recombination rate constants versus the $-\Delta G_{CR}$ values in the polar solvents.[33−35] The total reorganization energies have been determined to be $\lambda = 1.5-2.0$ eV in the solvent-separated radical ion pairs from the fitting the plots with the bell-shaped curves predicted by Sumi−Marcus[36] or Jortner−Bixon.[37] The good agreement of the boundary 1.8 eV with the total reorganization energies demonstrates that the exchange interaction is predominantly governed by the mechanism in Figure 6. This good agreement also demonstrates that the exchange interaction of the solvent-separated radical ion pair is detectable by the RPM CIDEP measurements.

McConnell[13] suggested that the triplet state $^3(A^{2-}\cdots D^{2+})$ of the pair of the doubly charged donor and acceptor, which lies energetically higher than the radical ion pair state, selectively stabilizes the triplet radical ion pair. Even though the energies of the $^3(A^{2-}\cdots D^{2+})$ states are not known, it is quite difficult to explain the inversion of the sign of J around $-\Delta G_{CR} = 1.8$ eV obtained in the case of the triplet precursor reactions. Moreover, Kollmar[32] suggested a highly symmetrical arrangement of the donor−acceptor complex is needed for the stabilization of the triplet radical ion pair. The anion and cation radicals are randomly orientated within the radical ion pairs and the solvated radical ion pair cannot have symmetrical structures at the distance where the magnitude of the J is comparable to the HFI in the liquid polar solvents. The McConnell mechanism cannot be applicable in the bimolecular electron transfer reaction systems in the liquid media.

(c) Prediction of the Magnitude of the Charge-Transfer Type Exchange Interaction. The model of the charge-transfer type exchange interaction in Figure 6 explains almost all of the results of the signs of the J. With this mechanism, magnitudes

of the J in the radical ion pairs are easily expected to be different with species of the donor−acceptor systems. The charge-transfer type exchange interaction is governed by the following parameters in the liquid media, distance-dependent electronic coupling matrix element, $-\Delta G_{CR}$ and λ. For example, in the triplet precursor reaction systems in Figure 6, a or b, the following secular equation is expressed with the linear combination of the basis wave functions of the singlet radical ion pair $^1\Psi(A^-D^+)$ and the ground state A−D pair $^1\Psi(AD)$ at the ion pair's equilibrium nuclear coordinate as

$$\begin{vmatrix} -\Delta G_{CR} - \epsilon & H_{el}(r) \\ H_{el}(r) & \lambda - \epsilon \end{vmatrix} = 0 \tag{8}$$

Here, $H_{el}(r)$ is the electronic coupling (CT interaction) between the radical ion pair and the ground state pair at the distance of r. The $H_{el}(r)$ is approximately proportional to the overlap between the highest occupied orbital of the donor and the lowest unoccupied orbital of the acceptor molecules. Therefore, $H_{el}(r)$ can usually be expressed in the form of exponentially decaying dependence on r as

$$H_{el}(r) = \left\langle {}^1\Psi(AD) \left| \frac{e^2}{r} \right| {}^1\Psi(A^-D^+) \right\rangle = H_0 \exp\{-\beta(r-d)\} \tag{9}$$

where H_0 denotes the electronic coupling matrix element at the contact separation (d). Assuming that the triplet radical ion pair is not perturbed through the electronic coupling, the singlet−triplet splitting in the radical ion pairs is expressed in the case of the weak-coupling electron transfer reaction system ($H_{el}(r) \ll \lambda + \Delta G_{CR}$) from eqs 8 and 9 as

$$J(r) = \epsilon + \Delta G_{CR} \approx -\frac{H_{el}(r)^2}{\lambda + \Delta G_{CR}} = -\frac{{H_0}^2}{\lambda + \Delta G_{CR}} \exp\{-2\beta(r-d)\} \tag{10}$$

From eq 10 the distance dependence of the charge-transfer type exchange interaction is similar to the dependence of electron transfer reaction probability[35] derived from the electron transfer reaction theory. Magnitudes of the J are predicted at the distance ($r = r_{SSRIP}$) of the solvent-separated radical ion pairs. $H_{el}(r_{SSRIP}) = 10\ cm^{-1}$, and $\lambda = 15\,000\ cm^{-1}$ (1.8 eV) at $r_{SSRIP} = 7-8$ Å,[35] yield the magnitudes of the J estimated to be $J(r_{SSRIP}) = -0.029\ cm^{-1}$, and $+0.024\ cm^{-1}$ in the *N*-methylphenothiazine-1,2,4,5-TCNB ($-\Delta G_{CR} = 1.37$ eV) and in the *N*-methylphenothiazine−1,4-DCNB ($-\Delta G_{CR} = 2.32$ eV) radical ion pairs in Figure 5, respectively. From the charge-transfer type exchange interaction, the absolute value of the J is predicted to be quite smaller than the electronic coupling in the donor−acceptor system. The predicted magnitudes of J are consistent with a relatively small magnitude of J in a radical−triplet pair, when the triplet quenching reaction is dominated by the CT interaction.[5c,38]

Studies on solvent polarity and temperature effects on the J in radical ion pairs are now under the progress.

Conclusion

We have demonstrated that the energy splitting between the singlet and triplet radical ion pairs is generated by the spin-selective electronic coupling perturbed from the both singlet and triplet charge recombined donor−acceptor states in the bimolecular electron transfer reaction system. It has especially been proved that the configuration change in the ensemble of solutes and solvent molecules caused by the electron transfer has a quite important role for the charge-transfer type exchange interaction. This mechanism is similar to the treatment for the analysis of the electron transfer reaction probability based on the electron transfer reaction theory. On the other hand, in neutral radical pairs, exchange interaction can be explained in terms of the Heitler−London model. The exchange integral governs the exchange interaction with a concept that the singlet radical pair is stabilized and makes a new chemical bond in their recombination process. The Heitler−London model is not applied to the radical ion pairs because they do not make new chemical bonds in their recombination processes but yield singlet and triplet donor−acceptor pairs by the back electron transfer reactions.

Acknowledgment. This work was supported in part by a Grant-in-Aid of Science Research No.09740537 from the ministry of Education, Science, Sports and Culture, Japan.

Supporting Information Available: Additional experimental details. This material is available free of charge via the Internet at http://pubs.acs.org.

References and Notes

(1) Adrian, F. J. *Rev. Chem. Intermed.* **1979**, *3*, 3.
(2) Alexander, M. H.; Salem, L. *J. Chem. Phys.* **1967**, *46*, 430.
(3) (a) Kaptain, R.; Oosterhoff, J. L. *Chem. Phys. Lett.* **1969**, *4*, 195. (b) Muss, L. T.; Atkins, P. W.; McLauchlan, K. A.; Pedersen, J. B. *Chemically Induced Magnetic Polarization*; Reidel: Dordrecht, 1977.
(4) (a) Kawai, A.; Okutsu, T.; Obi, K. *J. Phys. Chem.* **1991**, *95*, 9130. (b) Kawai, A.; Obi, K. *J. Phys. Chem.* **1992**, *96*, 52. (c) Kawai, A.; Obi, K. *J. Phys. Chem.* **1992**, *96*, 5701.
(5) (a) Kobori, Y.; Kawai, A.; Obi, K. *J. Phys. Chem.* **1994**, *98*, 6425. (b) Kobori, Y.; Mitsui, M.; Kawai, A.; Obi, K. *Chem. Phys. Lett.* **1996**, *252*, 355. (c) Kobori, Y.; Takeda, K.; Tsuji, K.; Kawai, A.; Obi, K. *J. Phys. Chem. A* **1998**, *102*, 5160.
(6) Batchelor, S. N.; Heikkilä, H.; Kay, C. W. M.; McLauchlan, K. A.; Shkrob, I. A. *Chem. Phys.* **1992**, *162*, 29.
(7) Murai, H.; Kuwata, K. *Chem. Phys. Lett.* **1989**, *164*, 567.
(8) Jeevarajan, A. S.; Fessenden, R. W. *J. Phys. Chem.* **1992**, *96*, 1520.
(9) Sekiguchi, S.; Akiyama, K.; Tero-Kubota, S. *Chem. Phys. Lett.* **1996**, *263*, 161.
(10) (a) Sekiguchi, S.; Kobori, Y.; Akiyama, K.; Tero-Kubota, S. *J. Am. Chem. Soc.* **1998**, *120*, 1325. (b) Kobori, Y.; Sekiguchi, S.; Akiyama, K.; Tero-Kubota, S. *Proceedings of the Joint 29th AMPERE−13th ISMAR. International Conference on Magnetic Resonance and Related Phenomena*; 1998; Vol. II, p 929.
(11) (a) Prisner, O.; Dobbert, O.; Dinse, K.-P.; van Willigen, H. *J. Am. Chem. Soc.* **1988**, *110*, 1622. (b) Kroll, G.; Plüschau, M.; Dinse, K.-P. *J. Chem. Phys.* **1990**, *93*, 8709.
(12) Avdievich, N. I.; Jeevarajan, A. S.; Forbes, M. D. E. *J. Phys. Chem.* **1996**, *100*, 5334.
(13) McConnell, H. M. Proceedings of the 11th Robert A. Welch Foundation Conference on Chemical Research; 1967; p 144.
(14) Volk, M.; Häberle, T.; Feick, R.; Ogrodnik, A.; Michel-Beyerle, M-E. *J. Phys. Chem.* **1993**, *97*, 9831.
(15) (a) Marcus, R. A. *J. Chem. Phys.* **1956**, *24*, 966. (b) Marcus, R. A. *J. Chem. Phys.* **1956**, *24*, 979.
(16) Kavarnos, G. J.; Turro, N. J. *Chem. Rev.* **1986**, *86*, 401.
(17) Shushin, A. I. *Chem. Phys. Lett.* **1991**, *183*, 321.
(18) Shkrob, I. A. *Chem. Phys. Lett.* **1996**, *264*, 417.
(19) Batchelor, S. N.; Kay, C. W. N.; McLauchlan, K. A.; Shkrob, I. A. *J. Phys. Chem.* **1993**, *97*, 13250.
(20) Kikuchi, K.; Hoshi, M.; Niwa, T.; Takahashi, Y.; Miyashi, T. *J. Phys. Chem.* **1991**, *95*, 38.
(21) (a) Akiyama, K.; Tero-Kubota, S. *Res. Chem. Intermed.* **1996**, *22*, 5334. (b) Akiyama, K.; Sekiguchi, S.; Tero-Kubota, S. *J. Phys. Chem.* **1996**, *100*, 180.
(22) Murov, S. L. *Handbook of Photochemistry*; Marcel Dekker: New York, 1993.
(23) Rehm, D.; Weller, A. *Isr. J. Chem.* **1970**, *8*, 259.
(24) Mann, C. K.; Barnes, K. K. *Electrochemical Reactions in Nonaqueous Systems*; Marcel Dekker: New York, 1970.
(25) Weil, J. H.; Bolton, J. R.; Wertz, J. E. *Electron Paramagnetic Resonance*; John Wiley and Sons: New York, 1994.
(26) Sakaguchi, Y.; Hayashi, H. *J. Phys. Chem. A* **1997**, *101*, 549.

(27) Rieger, P. H.; Bernal, I.; Reinmuth, W. H.; Fraenkel, G. K. *J. Am. Chem. Soc.* **1963**, *85*, 683.

(28) Leavanon, H.; Regov, A.; Galili, T.; Hugerat, M.; Chang, C. K.; Fajer, J. *J. Phys. Chem.* **1993**, *97*, 13198.

(29) (a) Katsuki, A.; Akiyama, K.; Tero-Kubota, S.; Ikegami, Y. *J. Am. Chem. Soc.* **1994**, *116*, 12065. (b) Katsuki, A.; Akiyama, K.; Tero-Kubota, S. *Bull. Chem. Soc. Jpn.* **1995**, *68*, 3383.

(30) Sasaki, S.; Katsuki, A.; Akiyama, K.; Tero-Kubota, S. *J. Am. Chem. Soc.* **1997**, *119*, 1327.

(31) Sekihara, A.; Honma, H.; Fukuju, T.; Maeda, K.; Murai, H. *Res. Chem. Intermed.* **1998**, *24*, 859.

(32) Kollmar, C.; Kahn, O. *J. Am. Chem. Soc.* **1991**, *113*, 7987.

(33) Kikuchi, K.; Niwa, T.; Takahashi, Y.; Ikeda, H.; Miyashi, T. *J. Phys. Chem.* **1993**, *97*, 5070.

(34) Mataga, N.; Asahi, T.; Kanda, Y.; Okada, T. *Chem. Phys.* **1988**, *127*, 249.

(35) Gould, I. R.; Young, R. H.; Moody, R. E.; Farid, S. *J. Phys. Chem.* **1991**, *95*, 2068.

(36) (a) Sumi, H.; Marcus, R. A. *J. Chem. Phys.* **1986**, *84*, 4272. (b) Sumi, H.; Marcus, R. A. *J. Chem. Phys.* **1986**, *84*, 4894.

(37) Jortner, J.; Bixon, M. *J. Chem. Phys.* **1988**, *88*, 167.

(38) Goudsmit, G. H.; Paul, H.; Shushin, A. I. *J. Phys. Chem.* **1993**, *97*, 13243.